Supporting Information For:

A 3D-Printed Microfluidic Microdissector for High-Throughput Studies of Cellular Aging

Eric C. Spivey[1,4], Blerta Xhemalce[1,3], Jason B. Shear[2,3*], and Ilya J. Finkelstein[1,3,4,*]

[1]Department of Molecular Biosciences, [2]Department of Chemistry and Biochemistry, [3]Institute for Cellular and Molecular Biology, [4]Center for Systems and Synthetic Biology, The University of Texas at Austin, Austin, Texas 78712

* Corresponding authors: J.B.S.: jshear@cm.utexas.edu; I.J.F: ifinkelstein@cm.utexas.edu

ABSTRACT

Due to their short lifespan, rapid division and ease of genetic manipulation, yeasts are popular model organisms for studying aging in actively dividing cells. To study replicative aging over many cell divisions, individual cells must be continuously separated from their progeny via a laborious manual microdissection procedure. Microfluidics-based soft-lithography devices have recently been used to automate microdissection of the budding yeast Saccharomyces cerevisiae. However, little is known about replicative aging in Schizosaccharomyces pombe, a rod-shaped yeast that divides by binary fission and shares many conserved biological functions with higher eukaryotes. In this report, we develop a versatile multiphoton lithography method that enables rapid fabrication of three-dimensional master structures for PDMS-based microfluidics. We exploit the rapid-prototyping capabilities of multiphoton lithography to create and characterize a cell-capture device that is capable of high-resolution microscopic observation of hundreds of individual S. pombe cells. By continuously removing the progeny cells, we demonstrate that cell growth and protein aggregation can be tracked in individual cells for over ~100 hours. Thus, the fission yeast lifespan microdissector (FYLM) provides a powerful on-chip microdissection platform that will enable high-throughput studies of aging in rod-shaped cells.

Table of Contents

1. Device Fabrication

Fabrication in PEGDA

We routinely use a low molecular weight (700 Da) polyethylene glycol diacrylate (PEGDA) for fabricating devices. Rose bengal (RB), which absorbs in the 500-550 nm range, acts as the photosensitizer. To generate high-resolution (~1 fL) voxels, we use a high peak power, 740 nm titanium:sapphire laser.[1,2] This voxel resolution can be achieved because multi-photon absorption, which has a very narrow absorption cross-section, is required to activate the RB at this wavelength.

We found that PEGDA has four advantages as a µ3D-printing material. First, PEGDA solutions can be prepared for fabrication using standard bench top equipment. In contrast, fabrication with SU-8 requires a chemical fume hood, spin coater, and access to other specialized clean room equipment.[3,4] Second, the densely cross-linked PEGDA structures do not warp or deform when transferred from water to ethanol or even when dehydrated. Third, PEGDA irreversibly cross-links to the surface of an acrylated microscope slide. This is a crucial requirement for any structure that will be used as a master for multiple rounds of PDMS-based soft lithography. Finally, this combination of PEGDA and RB is compatible with our 740 nm fabrication laser, the digital micromirror device (from a consumer-grade projector) and the scan mirror (from a confocal microscope). The optics in our rig were optimized for visible wavelengths, permitting a single setup to be used for both protein- and PEG-based fabrication.[5,6]

Capabilities of the Long Scan µ3DP System

The voxel size for all direct-write fabrication methods is governed by many factors including photosensitizer concentration, 2-photon action cross-section of the photosensitizer, wavelength of the laser, pulse width and peak energy of the laser and the numerical aperture of the objective. Below, we consider some addition considerations that are unique to the µ3D-printing method described in this manuscript.

Device width (x-axis):

In our current implementation, the maximum width of the fabricated structures (x-axis) is limited by the quality and magnification of the microscope objective. To produce wider structures, the beam is scanned through the objective at ever-larger angles. All objectives begin to act as lossy apertures at very large cone-angles, causing a decrease in the crosslinking efficiency.

Structures with a maximum width of ~120 µm could be fabricated with the 40x objective used in this study. However, Figure S3 shows that we could easily print up to three different FYLM variants side-by-side in one fabrication run. This permitted rapid prototyping of all FYLM dimensions. Using a 40x objective, each individually addressable mirror of the digital micromirror device (DMD) that served as our dynamic mask had a theoretical x-axis resolution of ~0.2 µm. As the smallest feature on the FYLM was larger than 1 µm (see Figure S2), we did not attempt to push our resolution beyond 1 µm.

Device length (y-axis):

The range of travel on the microscope stage limits the y-axis fabrication length and resolution. All the devices described in this manuscript (Figures 2B and S2) were ~0.5 mm long, but structures up to 2 mm long have been fabricated for other applications. The y-axis resolution is limited by the intensity of the excitation beam and the step-size of the microscope stage. According to the manufacturer's specifications, our stage is capable of making 100 nm steps. We did not attempt to produce features smaller than ~1 μm, the smallest size required by the FYLM device (see Figure S2).

Device height (z-axis):

The maximum height of our fabrication method is theoretically limited by the maximum z-travel available on the microscope stage. In the configuration described in this manuscript, it is limited by the working distance of the objective. The resolution is defined by the voxel size (see discussion above) and the step-size between progressive z-layers. For the FYLM device described in this manuscript, the fabrication scheme used a series of 20 vertical steps to produce a device that was 10 μm tall.

Comparison with Existing Methods

Our long scan μ3DP method combines the flexibility of dynamic mask-based μ3D printing[1,2,5] with the millimeter-length scales achieved by previous stage-scan methods.[3,4] Kumi et al. successfully fabricated master structures for centimeter-scale microfluidic channels with arbitrary cross-sections using SU-8 and a photoacid sensitiser.[3] Liu et al. used off-the-shelf SU-8 to fabricate millimeter-scale microfluidic microporous structures with a similar optical configuration.[4] We extended these long-range stage-scan methods by coupling them with our dynamic mask method. In the long scan μ3DP approach, the long axis (y-axis) features are encoded as movement of the microscope stage holding our substrate, while the short axis (x-axis) features are encoded as instructions for the DMD. By coordinating the microscope stage and the DMD, a single arbitrary layer can be fabricated. 3D structures such as those seen in figure S3 are built layer-by-layer at different z-axis locations. Thus, our long scan μ3DP method permits the fabrication of long branching structures with arbitrary cross-sections in all 3 dimensions.

Fabrication of SU-8 Re-Masters

Although the μ3D-printed PEGDA masters could be used immediately for generating PDMS flowcells, we found that the PDMS molds could also be filled with SU-8, allowing us to replicate a large set of new SU-8 masters from a single PEGDA-fabricated device. These SU-8 "re-masters" faithfully replicated the feature sizes of the original PEGDA masters and could be used as subsequent masters for PDMS flowcell construction. Furthermore, the SU-8 re-masters could be laminated with off-the-shelf dry film photoresists[7] for prototyping the FYLM with different flow schemes and cell-loading protocols. The fabrication protocol for making SU-8 re-masters is described below and summarized in supplemental figure S1.

PDMS molds for making SU-8 re-master structures were prepared by first mixing PDMS prepolymer and hardener (Dow Sylgard 184) at a 10:1 weight ratio for 30 min on a rotating mixer. The mixed polymer was then centrifuged at 1500 rpm for 90 s to remove large air bubbles. Master structures were placed in a shallow container and covered with ~5 g of liquid PDMS (Figure S1, step 1). The filled container was placed in a vacuum chamber and degassed under vacuum (~630 mm Hg) for ~15 min to remove air bubbles. The PDMS was cured overnight (14-20 h) at 60˚C.

Once cured, the PDMS mold was trimmed at the edges to ensure a flat surface (Figure S1, step 2). Glass slides (3" x 1"; Fisher) were cleaned with 2% liquid detergent (Hellmanex III; Helma Analytics) followed by a rinsing in water and isopropanol before drying at 60 ˚C on a hot plate. The PDMS mold was then placed over a cleaned glass slide, separated by 300-µm-thick PDMS spacers. SU-8 2010 (Microchem) was warmed to 40 ˚C in a water bath to reduce viscosity, then 700 µL was injected into the space between the PDMS mold and the glass over a 10-min. period (Figure S1, step 3). The slide with the SU-8 and PDMS mold was placed into a gel-imaging transilluminator (SynOptics InGenious) and exposed to near-UV light for 30 min. The PDMS mold was then removed, leaving a high-fidelity re-master structure on the glass slide (Figure S1, step 4). Edges of the re-master were then trimmed to ensure a flat lamination surface.

To produce the ~1-mm-wide flow channels that interface with the microfluidic device, a 3" x 1" strip of dry-film resist (DuPont MX5050) was laminated onto a re-master structure using an office laminator (ProLam Photo Pouch Laminator) at a rate of 14 mm s^{-1} at 95 ˚C. After lamination, the slide was heated for 80 s on a 95 ˚C hot plate prior to UV exposure. The protective polyester film was then removed from the resist and a mask aligner (Karl Suss MA6) was used to align the interface mask with the re-master structure. The film was exposed through a photomask (CAD/Art Services) at a power density of 130 mW cm-2 with a peak wavelength of 315 nm. The slide was then heated for 60 s at 95˚C before being developed. The UV-cured resist was developed with 60 s of gentle agitation in a bath of 1% potassium carbonate, followed by an isopropanol rinse. This cycle was repeated 4 times, after which the developed slide was dried using clean nitrogen gas.

2. Loading Cells Into the FYLM

The FYLM was filled with ~150 µL of filtered 70% EtOH. All tubing and valves (IDEX Health and Science) and the injection port of a manually-actuated 6-way injection valve (Cheminert C22-3186, Vici) were sonicated for 20 min in 2% Helmannex, then rinsed with deionized water and sonicated for 20 min in 70% EtOH. Parts were rinsed with EtOH and dried on a hot plate or oven at 70 ˚C. Parts were connected to 1/16" OD PFA tubing (IDEX 1512), then flushed with 70% EtOH with all valves open. A syringe (309650, BD Biosciences) containing 30 mL of 0.2 µm filtered (25-244 Olympus Plastics) YES media (Sunrise Science Products) was placed in a syringe pump (Legato 210, KD Scientific). After purging air bubbles from the tubing, flow was halted. The interface tubing was then connected to the nanoports on the FYLM, taking care not to introduce air bubbles into the device. Flow was started again to remove all remaining 70%

EtOH from the system. In all, ~1 mL of YES was flushed through all sections of the system to ensure that the FYLM was prepared for cell loading.

Log phase *S. pombe* cells were grown overnight at 30˚C in YES medium to an OD600 < 1.0. Cells were filtered through a 20 µm filter (SCNY00020; Millipore Steriflip) to remove any large clumps of cells or debris that could cause a blockage in the FYLM. 3 mL of cells were centrifuged at 3000 RPM for 3 minutes, then half of the supernatant was removed from each tube and cells were resuspended in the remaining YES.

Figure S4 summarizes the fluidic interface for the FYLM device. Concentrated cell solution was drawn into a sterile 1 mL syringe (309659, BD Biosciences) and attached to (closed) V3 of the interface (Figure S4). V1 and V2 were opened, and the syringe pump was started at 20 µL min^{-1}. After ~1 minute, V3 was opened and ~100 µL of the cell solution was injected into the FYLM (Figure S4, Step 1). Cell loading was monitored on the microscope. After the catch channels were filled with cells, V3 was closed and the cell syringe was removed. V3 was then reopened, V2 was closed, and the tubing flushed for 15 minutes (Figure S4, Step 2). Flow was reduced to 2 µL min^{-1} gradually (over 10 minutes) to reduce backflow in the FYLM. Flow was then maintained at 2 µL min^{-1} for the remainder of the experiment (Figure S4, Step 3).

In experiments where cells were dosed with YES media containing 1 mM H_2O_2, V3 was closed and V2 reopened, while the 20 µL loop on the injection device was loaded with the H_2O_2 solution. V1 was then closed and the injection port was then switched to the injection position for 10 minutes (Figure S4, Step 4) before being switched back to load position.

3. Characterizing Growth Within the FYLM

To rule out that cell growth was not perturbed within the FYLM, we compare the division times of both trapped and free cells. Figure S6 shows a summary of the results. Using the procedure described in Section 2 above, we measured the division times of cells subjected to media flow in the catch channels. This data was also used to make the histogram in Figure 5A. For cells subjected to flow outside of the catch channels, the same loading procedure was followed, except that the FYLM was not purged. This ensured that free cells were present throughout the device. Additional fields of view were acquired upstream of the FYLM to record the division of these free cells.

We also confirmed that the perfusion of fresh media does not adversely affect cell growth. For cells not subjected to media flow, the procedure described in Section 2 above was used, except that the FYLM was not purged after loading, the syringe pump was halted, and all valves were closed for the duration of the experiment.

For all cases, a two-minute time-lapse acquisition was initiated. We manually noted the doubling times of all cells that divided at least two times. The data in Figure S6 reports at least 50 observations for each growth condition.

4. Supplemental Figures

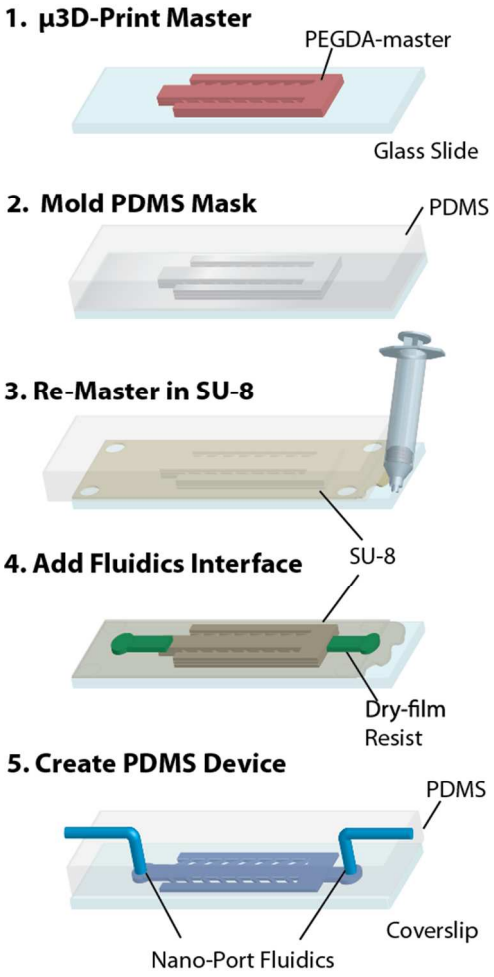

Figure S1. Process for creating a fluidic interface for the FYLM. (1) A master structure is µ3D-printed in PEGDA. (2) PDMS is then molded over the PEGDA structure. Master structure can be reused >3 times. (3) The PDMS mold is positioned with spacers above a glass slide and back-filled with SU-8. SU-8 is cured with UV light, creating a "re-master" of the original FYLM. (4) A dry-film photoresist is applied to the SU-8 re-master using an office laminator, then a low-resolution (>10 µm features) transparency mask is used to pattern a fluidic interface around the FYLM (shown in green). (5) A complete FYLM device is molded with PDMS. Once cured, the PDMS is removed from the re-master and plasma bonded to a cover slip. By creating several SU-8 "re-masters" from a starting PEGDA structure, we can rapidly produce multiple microfluidic devices in parallel.

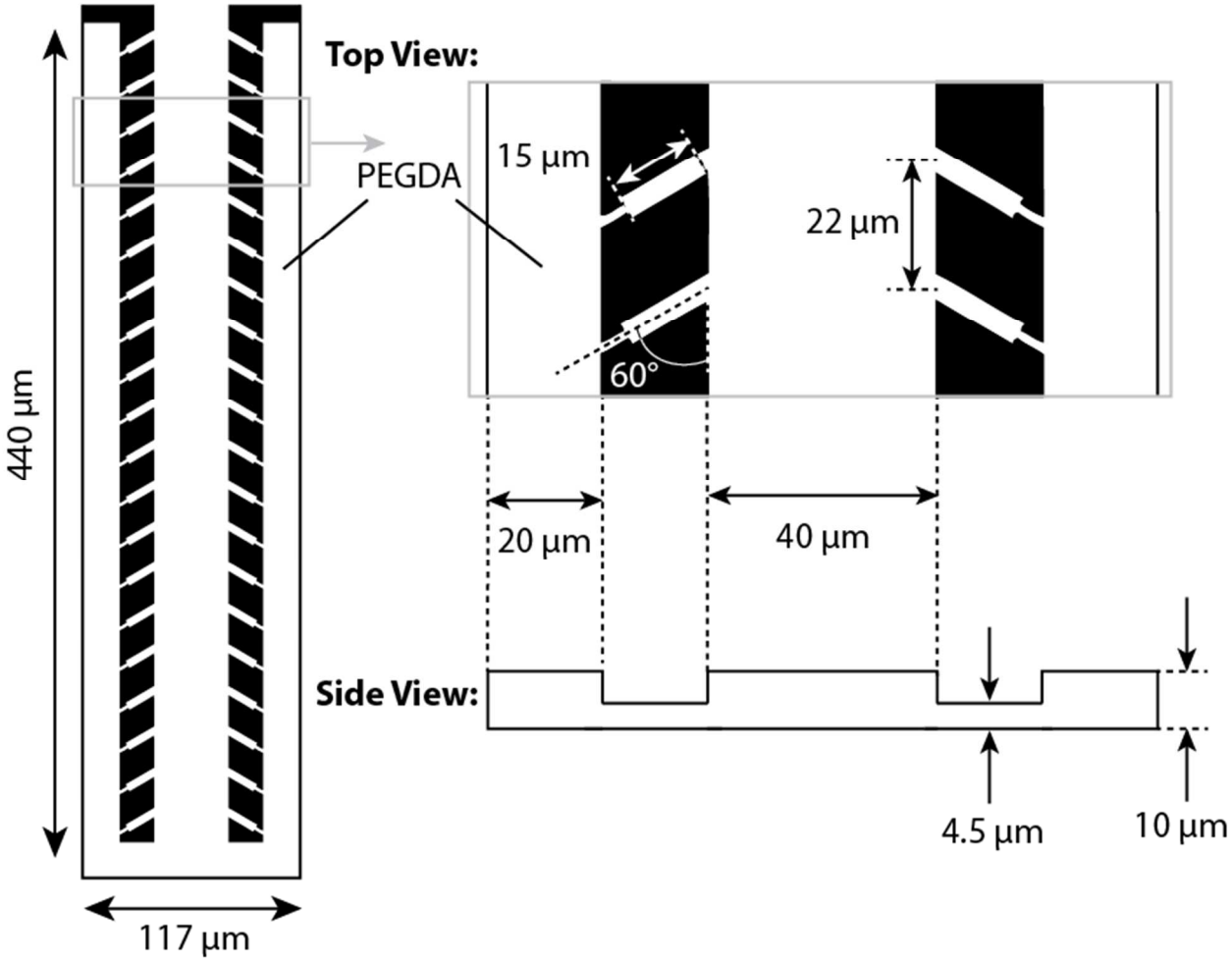

Figure S2. A schematic of the FYLM device showing a 60˚ device. Measurements were identical for 45˚ and 90˚ devices, except for the angle of the catch channel (45˚ and 90˚ respectively.

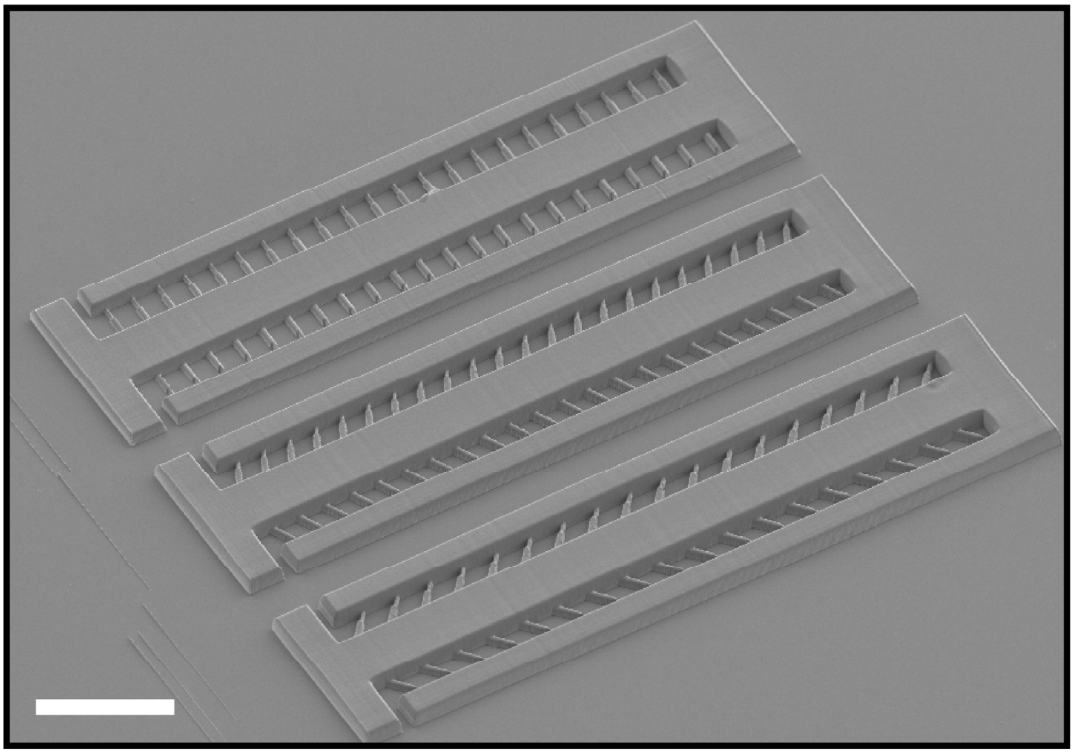

Figure S3. SEM image of three FYLM devices with catch channels oriented at 90˚, 60˚, and 45˚ relative to the central trench. The three devices were fabricated in PEGDA during a single fabrication run as described in the Supplemental Methods above. Total fabrication time was less than 45 minutes for all three devices. Scale bar is 100 μm.

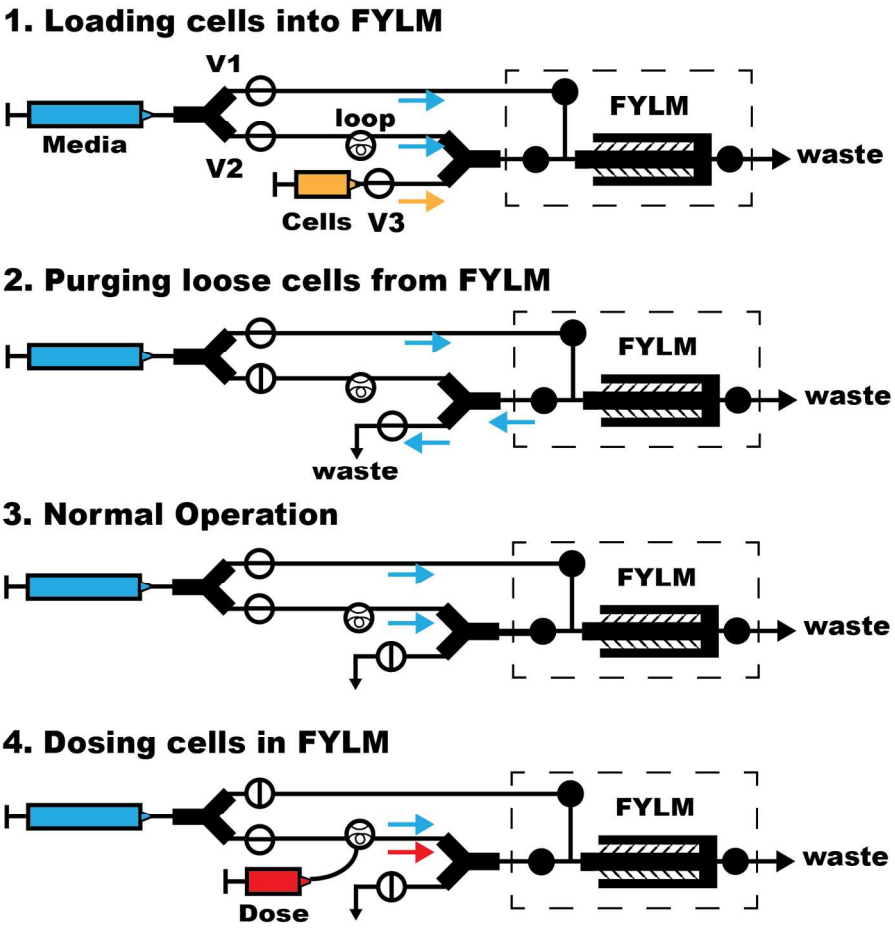

Figure S4. A schematic illustration showing steps for loading and operating the FYLM. Lines represent PEEK tubing (IDEX Health & Science). Arrows show direction of flow during different phases of operation. Dark circles represent Nanoports on the FYLM. Bisected circles represent valves (V1-V3) with lines parallel to tubing representing open valves, and lines perpendicular to tubing representing closed valves. "Loop" represents a manually-actuated injection loop used for dosing cells. 1) To load cells, the FYLM is first flushed out with filtered YES media. Then, ~100µl of cells (at an OD_{600}~1.0) is injected via a manually operated syringe connected to V3. 2) To reduce the accumulation of uncaught cells, V2 is closed, the cell-loading syringe removed, and the cell-loading tubing is flushed for a few minutes with YES media. 3) Constant flow through the FYLM is established once the tubing has been purged. Sufficient flow can be established with either V1 or V2 open, but leaving both open reduces the occurrence of air bubbles. 4) Cells can be treated with drugs by filling the injection loop with the desired dose (e.g. YES + H_2O_2). Changing the length of the injection loop defines the length of the treatment.

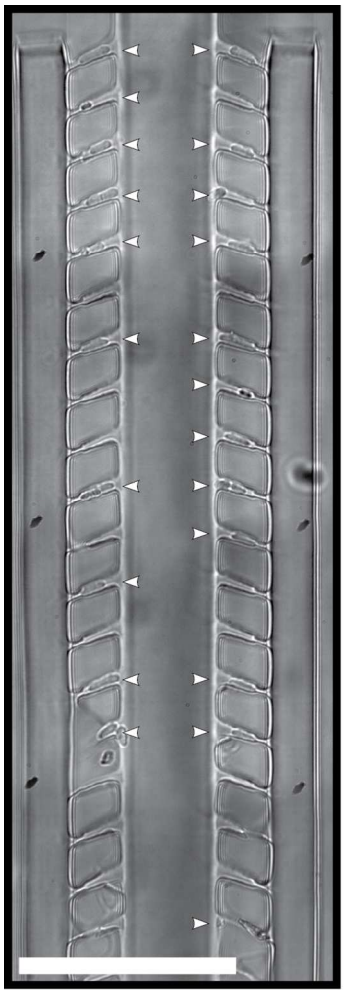

Figure S5. A FYLM device with 4 µm-wide catch channels was loaded with *S. pombe* cells. This image was formed by stitching six optical fields-of-view together.[8] Single cells can be seen in ~50 % of the catch channels (marked with white triangles). The loading efficiency did not depend appreciably on the angle of the catch channels. Scale bar is 100 µm.

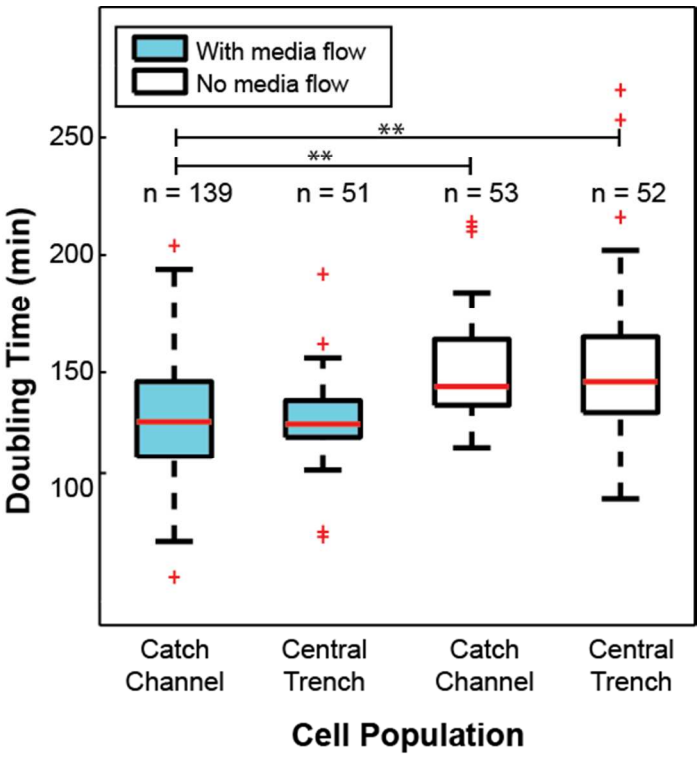

Figure S6. *S. pombe* cells exhibit robust growth in the FYLM. The box plots summarize the distribution of doubling times for cells immobilized in the catch channels or free within the central trench. In the presence of media flow, cells could freely flow through the central trench. However, we scored the doubling times of freely flowing cells that are transiently captured on minor PDMS imperfections. For each distribution, the red line indicates the median doubling time. The edges of the box report the first and third quartiles of the distribution, with the whiskers indicating the 5% and 95% confidence intervals. Individual outliers are marked with red plus symbols. The number of cell replication events measured for each condition is indicated above each box. There was no statistical difference between the doubling times of cells grown with the perfusion of fresh media (blue boxes; p-value: 0.6). In the absence of fresh media (white boxes), cells doubled more slowly (** denotes $p < 0.01$). Without media flow, the cells rapidly clogged the nano-fluidic device (within ~4 generations). Thus, we conclude that a gentle perfusion of fresh media stimulates robust growth within the catch channels. All further experiments were conducted in the presence of media flow. A summary of these results is also included in Table S2.

Video S1. Process for generating dynamic masks for µ3DP. A FYLM design is rendered as a stack of 2D masks, where each 2D mask represents a fabricated layer of the final FYLM. Each 2D mask is translated to a timed sequence of linear masks. The linear masks are displayed on the DMD and scanned with the fabrication laser. Synchronized movement of the microscope stage translates the PEGDA substrate, fabricating a continuous layer of the FYLM master. After each

layer is complete, the fabrication beam is shuttered, stage movement stops, and the stage is stepped along the optical axis, after which the process is repeated for the next layer.

Video S2. Continuous observation of cells dividing for over 90 hours. Cells were loaded in the FYLM device and fresh media was introduced at a rate of 2 μL min^{-1}. The top cell continued to divide for the duration of the movie (43 generations), whereas the lower cell ceases to divide after ~78 hours (36 generations). These movies clearly demonstrate that we can continuously observe individual cells within the FYLM.

Video S3. Observation of cells after H_2O_2 treatment. Cells were loaded in the FYLM device then treated with YES containing 1 mM H_2O_2 as described in Figure S4. YES + 1 mM H_2O_2 was injected into the system at the 3:47 (hh:mm) time, with the flow rate set to 2 μL min^{-1}. At this flow rate, the H_2O_2 solution required ~20 minutes to travel from the injection point to the cells. Numerous bright Hsp104-GFP puncta are visible by 4:26. Puncta form a large, bright aggregate that localizes at the old pole end of the cell (Hsp104 is also enriched as the nucleus, seen as a faint fluorescent mid-cell signal). At 17:02, the large aggregate appears to be displaced to the new pole end by an unknown mechanism. Note that several of the sister cells appear to die shortly after cell division.

5. Supplemental Tables

Table S1. *S. pombe* strains used in this study.

Name	Genotype	Source
L972	Wild-type h-	Leupold (1970)
DN111	h- hsp104-GFP-S65T:kan	Nilssen and Sunnerhagen (2011)

Table S2. Cell doubling times within the FYLM.

Cell Population[1]		Mean doubling time ± standard deviation (minutes)
Catch Channel (N=139)	With fresh media flow	131 ± 25
Central Trench (N=51)		130 ± 18
Catch Channel (N=53)	No media flow	152 ± 23
Central Trench (N=52)		152 ± 33

6. References

(1) Ritschdorff, E. T.; Nielson, R.; Shear, J. B. *Lab. Chip* **2012**, *12*, 867–871.

(2) Spivey, E. C.; Ritschdorff, E. T.; Connell, J. L.; McLennon, C. A.; Schmidt, C. E.; Shear, J. B. *Adv. Funct. Mater.* **2013**, *23*, 333–339.

(3) Kumi, G.; Yanez, C. O.; Belfield, K. D.; Fourkas, J. T. *Lab. Chip* **2010**, *10*, 1057.

(4) Liu, Y.; Nolte, D. D.; Pyrak-Nolte, L. J. *Appl. Phys. A* **2010**, *100*, 181–191.

(5) Nielson, R.; Kaehr, B.; Shear, J. *Small* **2009**, *5*, 120–125.

(6) Jhaveri, S.; McMullen, J.; Sijbesma, R.; Tan, L.; Zipfel, W.; Ober, C. *Chem. Mater.* **2009**, *21*, 2003–2006.

(7) Robison, A. D.; Finkelstein, I. J. *Anal. Chem.* **2014**, *86*, 4157–4163.

(8) Preibisch, S.; Saalfeld, S.; Tomancak, P. *Bioinformatics* **2009**, *25*, 1463–1465.